Novembre 1984 INT 117/84

ALFVEN WAVE HEATING IN TCA 1981 - 84

compiled by

G.A. Collins, J.B. Lister

This note is extracted from the FN 3-year report (1984) and summarizes the AWH results obtained in that period. The boundary physics section was written by F. Hofmann, Ch. Hollenstein.

Centre de Recherches en Physique des Plasmas
Association Euratom - Confédération Suisse
Ecole Polytechnique Fédérale de Lausanne

1. INTRODUCTION

The TCA tokamak was constructed during the previous 3-year period and its operation with rf wave studies had just begun at the time of the last report. The activity over the last 3 years has concentrated primarily on advancing the understanding of the physics behind Alfvén Wave Heating (AWH), and on achieving rf-heated plasmas. We recall that the main parameters of the tokamak are :

Toroidal magnetic field	15 kGauss
Major radius	61 cm
Minor radius	18 cm
Maximum plasma current	$\leq$170 kA
Duration of the current plateau	$\leq$160 ms
AWH generator frequency	2.5 MHz
Plasma density $(n_e(0))$	$\leq 1.5\times10^{14}$ cm^{-3}
$T_e(0)$ (ohmic)	$\leq$850 eV
$T_i(0)$ (ohmic)	$\leq$350 eV

As well as the permanent team on TCA, there are several collaborative projects around the tokamak, namely :

- The University of Zürich (Dr. S. Veprek) is involved with experiments on plasma wall interactions in TCA [48,83,174].
- The University of Fribourg (Prof. H. Schneider) has built a radiation detector [119,138] which is being used for bolometric measurements in TCA, and a multi-channel version is being commissioned.
- The Intitut de Génie Atomique (EPFL) has started studying the effect of bombardment by energetic neutral atoms on samples inserted in the tokamak.
- Other institutes at the EPFL are collaborating in surface studies of the limiters used in TCA, coordinated by Prof. Martin.
- Culham Laboratory (UKAEA) is presently collaborating on a study of SiC coated limiters.
- Culham Laboratory (UKAEA) has collaborated on an initial spectroscopic survey of the TCA plasma, in the VUV range of the spectrum [T1,31,137,168].

In the paragraphs which follow, we shall discuss improvements made to the tokamak experiment, including diagnostics, and then describe the physics milestones reached during this 3-year period.

2. IMPROVEMENTS TO THE EXPERIMENTS

2.1 Operational

The main improvement to the TCA operation was the addition of an active control of the plasma current during the current flat-top phase. This was achieved using a variable switched-resistor system, similar to that used on the vertical field system, constructed in-house. This system allows a preprogrammed current waveform to be produced using feedback control over the plasma column loop voltage. Coupled with a reduced value of the required loop-voltage (see section 4) the controlled pulse length has reached 160 msec before the plasma current decays gently. We have also commissioned a feedback loop to control the plasma density, using the 2 mm interferometer. These two feedback loops have allowed very simple yet very flexible operation of TCA, and a typical shot obtained in these conditions is shown in Fig. 1. In Fig. 2 we show the operation diagram of TCA, obtained at 11.6 kG, in which we see that the range of operation has been extended to $q<3$ [148] and to values of n_eR/B_T up to 4.3×10^{19} Weber^{-1}.

In addition, we have constructed an increased ohmic-heating power supply, doubling the previous capacitor bank, and we have constructed a capacitor bank to allow us to reverse the primary current, thereby prolonging the plasma current. The vertical field power supply was also doubled to cater for the improved ohmic supply. These new supplies have not yet been fully commissioned.

3. RF COUPLING STUDIES

At the time of the previous report the first low power rf experiments on TCA had confirmed the parametric dependence of the antenna loading predicted by ideal mhd theory, but had also surprisingly revealed the existance of discrete resonances [11,116]. This discovery has since led to a rich variety of physics studies which can be summarized as follows :

3.1 Discrete Alfvén Waves

The discrete resonances have been identified as global eigenmodes of the Alfvén Waves, which although not important in the context of ideal mhd and cylindrical geometry, have been known to exist for many years at frequencies close to ω_{ci}.Their appearance in TCA at relatively low values of ω/ω_{ci} ~ .1-.3 has since been explained by the curvature of the magnetic field due to the equilibrium current. We observe that the eigenmodes (hereafter called Discrete Alfvén Waves or DAW's) only occur if the wave vector has the same sign of helicity as the equilibrium magnetic field, i.e. $n/m > 0$, where n and m are the toroidal and poloidal wavenumbers respectively. They occur at a frequency just below the start of the continuum associated with the corresponding Alfvén resonance layer. By varying plasma parameters over as wide a range as possible we have been able to identify DAW's with n ranging from 0 to 6 and to investigate their behavior in detail [59,67]. In Fig. 5 [59] we show how the value of plasma parameters at which the DAW's are excited depends on the plasma current. This has suggested their use as a diagnostic tool to measure in particular the mass density ρ and safety factor q near axis. The coupling to the resonance peaks associated with the DAW's and to the continua has also been studied and in Fig. 6 [59] we see how the plasma current assists in the coupling to both. The enhanced antenna loading associated with a DAW suggests that they might be used for plasma heating and current drive, particularly since they are characterised by large amplitudes near the axis. However, unlike the continuous loading, their usefulness for heating depends on the damping mechanism and they suffer from being natural modes of the plasma, with large amplitude at the edge of the plasma.

3.2 Ion Cyclotron Effects and Mode Identification

Triple magnetic field probes in the shadow of the limiter have been used to help identify the various modes excited in the plasma, and in particular to investigate the interference between the DAW's and the continua which have different n and m numbers [44,142]. These studies have shown that modes with m negative are dominant in the plasma, consistent with recent theoretical work attributing this to ion cyclotron effects on the highly damped compressional (or fast magnetosonic) waves excited by the antenna. In our case these are the so-called "surface" waves which act as energy carrier to the Alfvén resonance layer and enhance the excitation of the DAW's. The splitting between m positive and negative, so that the surface wave eigenfrequency is only slightly above the threshold of the corresponding continuum for $m < 0$, occurs at very low values of ω/ω_{ci}, as confirmed by the experiment [82].

This effect also implies that in any given region of the spectrum a particular direction of propagation is preferred. Experimentally we have studied this by adjusting the phasings of the N=1 antenna to excite waves with a predetermined toroidal direction, Fig. 7 [101]. Due to the preference for $m < 0$, the $(n,m)=(-1,-1)$ DAW is more easily excited than the $(1,1)$ DAW even though they have the same helicity and are degenerate in ideal mhd. If the DAW's impart momentum to the electrons then their use for current drive is enhanced by the fact that they are more easily excited in the electron drift direction $(n<0)$.

3.3 Modulation of Coupling by mhd Activity

A closer examination of both the antenna loading and vacuum wavefields associated with the DAW's revealed that they were modulated in amplitude synchronously with both island rotation at frequencies $f \sim 10-15$ kHz, as seen on the poloidal field modulation and soft X-ray emission modulation, and with the sawteeth seen on the soft X-ray emission signals. We have explained this by the modulation of the resonance frequency since the profiles of ρ and q are themselves modulated by the mhd activity. In particular we have used the sawtooth modulation of the resonance peaks to study fast fluctuations in the current profile during the internal disruptions associated with the sawteeth [15,160]. The relative phase between the sawteeth seen on the soft X-ray flux and those on the DAW peaks provides information on the shape of the Alfvén frequency profile.

3.4 Observations of Toroidal Coupling

In addition to the (n,m) modes lauched by our antenna we have recently observed other modes present in the plasma. In particular an N=2, M=1 antenna couples well to both a DAW and continuum which correspond to (n,m)=(2,0) [87,101]. This observation is not only surprising because the antenna has only parasitic m=0 component but because direct excitation of the mode by an N=2, M=0 antenna proved impossible. In Fig. 8 [101] we compare the measured antenna loading with a one-dimensioned calculation. The new mode with its DAW and subsequent continuum can only be explained by consideration of the toroidal geometry. It is of importance because it is in this region of the spectrum that the majority of our heating experiments have been performed and because crossing the (2,0) continuum threshold has a dramatic effect on the macroscopic heating behaviour (see Section 6). Other toroidally coupled modes have now been identified (2,2) and (4,0), always with poloidal wavenumber $m\pm1$, where m is the poloidal wavenumber of the principal directly excited mode. These observations stress the importance of the toroidal geometry in any consideration of AWH.

3.5 Dependence on the Edge Plasma

Initially the antennae were equipped with lateral screens which acted as particle shields. They were removed because they diminished the antenna-plasma coupling by perturbing the magnetic field structure. By controlling the vertical position of the plasma we were able to measure the coupling dependance on the antenna-plasma separation, Fig. 9 [59]. The D.C. potential of the antenna has been measured and we observed that with 50 kW of rf approximately -25 V of polarization appears on the antenna. This can be related to changes in the edge plasma characteristics as described in section 5. Active polarization of the antennae produced a decrease in the antenna loading, Fig. 10a) [86,148A] but surprisingly the vacuum wave-field measured by the magnetic probes actually increased for polarisation Voltages lower than -60V. A similar decrease in antenna loading was observed as a function of rf power (Fig. 10b)), although there is a saturation in the decrease near 100 kW corresponding roughly to the -60V of floating polarisation.

This is consistent with the picture of direct capacitive coupling to the edge plasma. The recent replacement of the lateral screens has completely removed these effects confirming that they were due to dissipation in the relatively high density scrape-off plasma near to the antennae.

4) IMPURITY REDUCTION

The original experiments with rf heating showed an increase in the intensity of impurity radiation. By 1982, we were able to deliver ~130 kW of rf power to the plasma, and showed dramatic increases in the radiated power loss [A1,23,164]. We showed that this increase was attributable to metallic impurities, mainly iron [170]. As a result of these observation we carried out an extensive program of limiter design and material changes [43,81,178]. We also replaced the stainless steel plate antennae [60] by novel TiN-coated bar antennae [85]. Finally we inserted lateral screens coated with TiN and changed the graphite limiter to a silicon-carbide coated limiter. The results are summarized in Fig. 11 [105]. We see that the latest configuration has an immeasurably small radiated power loss on axis with 110 kW of rf power. We consider that a metallic impurity influx is no longer an important element of the plasma power balance [105]. The plasma resistance has dropped by a factor of ~4 during the period. We have carried out radiated power loss profile simulation using a mixture of impurities and are able to model adequately the measured profiles [81,168]. The VUV spectrometer proved to be extremely useful in following the variation in impurity content during these various changes in configuration.

We have been able to show up a correlation between the rf wavefield and the impurity line increase [105]. The Li-like lines CIV, NV and OVI, as well as low ionisation metallic impurity lines FeII, TiIII, all generally show an increase during the rf pulse. They have also shown up a considerable fine-structure during the crossing of a DAW. We find that the increment of the edge-line intensity is linear with respect to the antenna-current rather than to the rf power for

P_{rf} < 100 kW at a fixed position in the spectrum. When we vary the excited mode structure, we further find that the increase anti-correlates with the antenna current, hence also with antenna voltage and antenna near-field at fixed rf power Fig. 12 [105]. In fact, we see that the edge-line intensity increase correlates best with the amplitude of the poloidal component of the far-field wavefield. The origin of the increase and hence the mechanism responsible for the correlation is not confirmed. The increase may be partly due to an increase in edge temperature. This signal response is extremely rapid, and appear to be faster than the response following an injection of low-Z impurity. A density profile modification remains a possibility, but it would have to be highly structured radially. We therefore assume that the effect is mainly due to a change impurity flux. Since the wavefield itself shows discontinuous behaviour at the mode threshold, it is interesting to moot a connection between these results and the previously discussed discontinuous behaviour.

5) EDGE PHYSICS

5.1 Impurity Fluxes and Erosion

Impurity fluxes in the scrape-off layer have been measured during Alfvén Wave Heating. Collection probes, in conjunction with XPS (X-ray photon electron spectroscopy) surface analysis, are used to determine impurity fluxes and ion impact energies. During RF heating, the impurity fluxes are enhanced. Probe erosion due to impurity sputtering is clearly observed [48,83,174].

In order to study further the antenna-plasma interaction, several samples were fixed onto various antenna groups. After exposure to the plasma, the samples were removed and analysed at the Institute for Inorganic Chemistry of the University of Zurich. Analysis by XPS has shown that the surfaces parallel to the principal magnetic field and to the antenna are less contaminated. The main impurities are carbon, chromium, and iron, measured after about 300 discharges and with molybdenum samples. The weak contamination could be explained by either a weak flux of impurities in this direction, or by sputtering.

In order to determine whether the sputtering in this direction is important, molybdenum samples with a gold coating a few Å thick have been exposed to the plasma. These samples are being analysed at Zurich.

Other analyses are being made with SiC-coated carbon limiters. The limiter located at the outside of the tokamak has been removed after the first test period. It is being analysed at the Institute of Atomic Engineering of the EPFL by Prof. Martin's team. With an SEM (Scanning Electron Microscope), we hope to determine the uniformity of the SiC coating over different positions on the limiter. Afterwards, microanalysis will be used to study the chemical composition of this exposed layer, and the amount of impurities as a function of depth.

5.2 Edge Plasma Measurements

Edge plasma mesurements have been made using Langmuir probes. The first measurements were made in the presence of large, stainless-steel antennae. When the RF is applied, the results show that the scrape-off plasma is strongly perturbed. During the RF phase of the discharge, the electron density falls and the electron temperature increases, by nearly a factor of 2. Measurements made under similar conditions, but with the bar antennae coated with TiN, show that the influence of the RF on the scrape-off plasma is reduced. The reduction of the electron density is weaker, although the increase in the electron temperature is still present. In addition, a detailed analysis of the Langmuir probe characteristics shows that the scrape-off plasma during RF is non-Maxwellian.

The electrostatic probe measurements have demonstrated the existence of RF currents of the order of 10 Amps/cm^2. These RF currents exist even in the presence of recently-installed lateral screens. However, the increase of the electron temperature has been eliminated by these screens. All these results show the strong interaction of high power RF heating with the scrape-off plasma.

5.3 Effect of Lateral Screens

Measurements previously made in the edge plasma using the floating antenna potential, Langmuir probes and grounded probes showed up considerable changes during the rf pulse. Subsequently, we have placed solid lateral screens, coated with TiN, both sides of each antenna, ~5 cm from the edge of each group and extending to 1 cm outside the limiter radius, with the intention of reducing the rapid edge plasma diffusion along the field lines towards the antennae. The screens were placed far enough from the antenna so as not to perturb the direct antenna field at the plasma boundary.

We found four main results. Firstly, the non-linear increase in loading observed at low power [86] has been eliminated and the DC plasma-antenna hold-off resistance has increased by two orders of magnitude, strongly suggesting that we have achieved the large local reduction in edge plasma density intended. Secondly, the solid lateral screens, while not blocking the antenna current near-field, block the surface-wave wavefield and reduce the antenna loading by ~50% in agreement with our numerical estimates. The screens do in fact provide antenna image currents since the plasma surface wave effectively enhances the mutual between screens and antennae. The size of this effect has been computed by assuming that the screen is equivalent to an additional antenna whose current is given by minimizing the RF magnetic flux enclosed by the loop. An attempt is currently underway to compute the effect of slotted side screens. Thirdly, the edge plasma profiles of density and temperature remain unchanged outside the screens when the rf is applied at the 100-150 kW power level. Fourthly, we find a considerably smaller increase of the metallic impurity concentration during the rf pulse as determined from bolometric and spectroscopic data. The radiated power loss on axis under the standard conditions is now ~0.05 W/cm^3 during the rf pulse with the screens compared with ~0.2 W/cm^3 previously, agreeing with a reduction by a factor of 2-3 in the metallic impurity core lines. The line intensities from low-Z impurities have remained the same, and still increase during the rf pulse. The density increase due to the rf pulse, at fixed rf power, has remained practically unchanged.

6) RF HEATING EXPERIMENTS

As discussed in Section 4, a considerable improvement in plasma purity was critical in advancing the rf heating experiments. We achieved one goal early in 1984, delivering the maximum available generator power, 400 kW (Fig 13) [105] to a relatively high density plasma while maintaining sawtoothing activity. As plasma purity was improved, we were able to observe macroscopic changes to the plasma associated with the Alfvén Wave mode spectrum [43,87,101,105,178]. The plasma density increase undergoes a discontinuity at the (n,m)=(2,0) threshold (see Section 3) (Fig. 14) [105], depending sensitively on the uncontrollable parameters. We associate this behaviour with the change in power deposition profile which occurs when crossing into a new continuum.

As a result of the insertion of the lateral screens we found that, although the antenna near field was unperturbed, the surface wave was blocked, leading to a large reduction in antenna loading, by about 50%. Consequently, we were unable to deliver more than ~110 kW at the end of this period. Work is underway to get around the problem.

Nonetheless, even with this power level, the heating results were impressive. We obtained (Fig. 15) [105] increases in electron and ion temperatures of ~30%, rising to 1200 eV and 400 eV respectively. The plasma energy content, measured magnetically also showed a large increase. The plasma density similarly increased during the rf pulse, roughly doubling. The most marked improvement was to produce a reduction in the plasma column resistance during the rf pulse, a clear indication of bulk electron-heating.

The question whether the increase in ion temperature during the rf pulse corresponded to a direct transfer of rf power to the ions, or to a change in the electron-ion transfer power resulting from the density increase, attracted considerable effort. Early results [20,23,43,164,178] suggested a clear direct transfer. Subsequent experiment suggest that the increase may be attributable to an increase in electronion transfer via impurities. Until we achieve $T_i > T_e$ this will remain an open question.

The origin of the density increase also remains a serious question. The density increment for a given rf power has remained constant throughout the rf experiments, to within ±10%, even with new limiters, new antennae and the addition of screens. Recycling of impurities at the wall is one possibility, but impurity injection experiments do not suggest that the density increase is due to low-Z influx. It is difficult to assume that the hydrogen recycling increases, since the H_α + D_α measurements have failed to show an increase in ionisation rate. This question continues to be studied.

Finally we have constructed a simple 1-D transport code to analyze the newest data in which the radiated power does not dominate the power balance. We find that the energy deficit during the rf pulse, calculated assuming $n\chi_e$ is unchanged and that the profiles remain unchanged, is very close to the delivered rf power. This suggests that either the AWH deposition profile is favourable, or that the thermal losses are reduced during the rf pulse. This new approach will be continued.

FIGURE CAPTION

Figure 1 : TCA tokamak plasma pulse

Figure 2 : Operation diagram at 11.6 kG in D_2

Figure 5 : Location of the DAW resonance peaks in the n_e : q(a) diagram

Figure 6 : Variation of antenna coupling as a function of q(a)

Figure 7 : Dissymetry between waves excited preferentially in either toroidal direction

Figure 8 : Comparison between measured antenna loading and a cylindrical model calculation

Figure 9 : Variation in antenna loading as the plasma position is varied

Figure 10 : Effect of antenna polarization and the non-linear loading effect

Figure 11 : Radiated power loss with different limiters and antennae (15.1 kG, D_2, (N,M)=(2,1), P_{rf} ~ 100 kW, n_e ~ 2.3 x 10^{19} m^{-3})

Figure 12 : Correlations between impurity line intensity and the antenna-current or rf wavefield

Figure 13 : High power scan in which maximum available power was delivered (15 kG, D_2, 5 x 10^{19} m^{-3})

Figure 14 : Discontinuous behaviour observed when crossing a mode threshold

Figure 15 : Heating effects during the rf pulse (15.1 kG, D_2, (N,M) = (2,1))

REFERENCES

T1 N.J. Peacock, M.F. Stamp, J.D. Silver, Physica Scripta T8, 10 (1984)

11 A. de Chambrier, A.D. Cheetham, A. Heym, F. Hofmann, B. Joye, R. Keller, A. Lietti, J.B. Lister, A. Pochelon
Alfvén wave coupling experiments on the TCA Tokamak
Plasma Physics 24, 893 - 902, (1982)

15 A. de Chambrier, P.A. Duperrex, A. Heym, F. Hofmann, B. Joye, R. Keller, A. Lietti, J.B. Lister, A. Pochelon
Observation of fast current fluctuations during internal disruptions in TCA by using Alfvén wave diagnostics
Phys. Lett. 92A, 6, 279 - 282, (1982)

20 A. de Chambrier, A. Heym, F. Hofmann, B. Joye, A. Lietti, J.B. Lister, A. Pochelon, W. Simm
Mesure de température ionique par analyse de particules neutres dans TCA (Tokamak chauffage Alfvén)
Helvetica Physica Acta 55, 583 (1982)

23 A. de Chambrier, A.D. Cheetham, A. Heym, F. Hofmann, B. Joye, R. Keller, A. Lietti, J.B. Lister, A. Pochelon, W. Simm, J.L. Toninato, A. Tuszel
Alfvén wave experiments in TCA
Proc. 9ème Conférence Internationale sur la Physique des Plasmas et la Recherche concernant la Fusion Nucléaire Contrôlée, Baltimore-USA, Septembre 1982, IAEA 1983, Vol. III, p. 81 - 89

24	A. de Chambrier G.A. Collins A. Heym F. Hofmann Ch. Hollenstein B. Joye R. Keller A. Lietti J.B. Lister J.M. Moret S. Nowak J. O'Rourke A. Pochelon W. Simm	Etudes paramétriques des décharges ohmiques dans le tokamak TCA Helvetica Physica Acta 56, 951 (1983)
31	A. de Chambrier A. Heym F. Hofmann B. Joye R. Keller A. Lietti J.B. Lister P.D. Morgan N.J. Peacock A. Pochelon M.F. Stamp	Measurements of electron and ion heating by Alfvén waves in the TCA tokamak Plasma Physics 25, 1021 - 1036 (1983)
43	R. Behn A. de Chambrier G.A. Collins P.A. Duperrex A. Heym F. Hofmann B. Joye Ch. Hollenstein R. Keller A. Lietti J.B. Lister J.-M. Moret S. Nowak J. O'Rourke A. Pochelon W. Simm	Recent Alfvén wave heating results on the TCA Tokamak Plasma Physics and Controlled Fusion 26, 173 (1984)
44	A. de Chambrier G. Collins P.A. Duperrex Ch. Hollenstein R. Keller A. Lietti J. O'Rourke A. Pochelon W. Simm	Identification des modes d'ondes d'Alfvén Helvetica Physica Acta 57, 110 - 120 (1984)

48 F. Hofmann, Ch. Hollenstein, B. Joye, A. Lietti, J.B. Lister, A. Pochelon, J.K. Gimzewski, S. Veprek

Scrape-off measurements during Alfvén wave heating in the TCA tokamak
Journal of Nuclear Materials 121, 22 - 28 (1984)

52 P.A. Duperrex, Ch. Hollenstein, B. Joye, R. Keller, J.B. Lister, F.B. Marcus, J.M. Moret, A. Pochelon, W. Simm

Magnetic broadband turbulence measurements and ohmic confinement in the TCA Tokamak
accepted for publication in Physics Letters A

59 A. de Chambrier, A.D. Cheetham, A. Heym, F. Hofmann, B. Joye, R. Keller, A. Lietti, J.B. Lister, A. Pochelon, W. Simm, J.L. Toninato, A. Tuszel

Alfvén wave absorption studies in TCA
Proc. Third Joint Varenna-Grenoble International Symposium, Grenoble, France, Mars 1982, Vol. I, EUR 7979 EN, p. 161 - 172

60 A. de Chambrier, A.D. Cheetham, A. Heym, F. Hofmann, B. Joye, R. Keller, A. Lietti, J.B. Lister, A. Pochelon, W. Simm, J.L. Toninato, A. Tuszel

The antenna for Alfvén wave heating in TCA
Proc. Third Joint Varenna-Grenoble International Syposium, Grenoble, France, Mars 1982, Vol. III, EUR 7979 EN, p. 1117 - 1121

67 A. de Chambrier, A.D. Cheetham, A. Heym, F. Hofmann, B. Joye, R. Keller, A. Lietti, J.B. Lister, A. Pochelon, W. Simm, J.L. Toninato, A. Tuszel

Alfvén wave propagation and absorption in TCA
Proc. 1982 International Conference on Plasma Physics, Göteborg, Suède, Juin 1982, p. 131

71	A. de Chambrier A. Heym F. Hofmann B. Joye R. Keller A. Lietti J.B. Lister A. Pochelon W. Simm J.L. Toninato A. Tuszel	The technique of Alfvén wave heating in the TCA Tokamak Proc. 12th Symposium on Fusion Technology, Jülich, R.F.A., Septembre 1982, Vol 2, p. 1295 - 1300
81	R. Behn F. Hofmann Ch. Hollenstein B. Joye J.B. Lister S. Nowak J. O'Rourke A. Pochelon	A comparison between steel, carbon and TiC-coated limiters in the TCA Tokamak Proc. 11th European Conference on Controlled Fusion and Plasma Physics, Aachen, Fed. Rep. of Germany, September 1983
82	K. Appert R. Behn A. de Chambrier G.A. Collins P.A. Duperrex F. Hofmann Ch. Hollenstein B. Joye R. Keller A. Lietti J.B. Lister J. O'Rourke A. Pochelon W. Simm L. Villard	Experimental determination of ω/ω_{ci} effects in shear Alfvén wave excitation in TCA Tokamak Proc. 11th European Conference on Controlled Fusion and Plasma Physics, Aachen, Fed. Rep. of Germany, September 1983
83	J.K. Gimzewski S. Verprek F. Hofmann J.B. Lister A. Pochelon P. Groner	Impurity fluxes in the scrape-off layer of the TCA tokamak: effects of RF heating Proc. 11th European Conference on Controlled Fusion and Plasma Physics, Aachen, Fed. Rep. of Germany, September 1983
84	A. de Chambrier G.A. Collins P.A. Duperrex A. Heym F. Hofmann Ch. Hollenstein B. Joye R. Keller A. Lietti J.B. Lister F.B. Marcus J.-M. Moret S. Nowak A. Pochelon W. Simm S. Veprek	Alfvén wave heating on TCA Proc. 4th Int. Symposium on Heating in Toroidal Plasmas, Rome, Italy, March 1984, Vol. I, p. 137 - 152

85	A. de Chambrier G.A. Collins P.-A. Duperrex F. Hofmann Ch. Hollenstein B. Joye R. Keller A. Lietti J.B. Lister F.B. Marcus J.-M. Moret S. Nowak A. Pochelon W. Simm	Alfvén wave heating results in TCA using coated bar anteanne Proc. 4th Int. Symposium on Heating in Toroidal Plasmas, Rome, Italy, March 1984, Vol. I, p. 179 - 186
86	A. de Chambrier G.A. Collins P.A. Duperrex M. Grossmann A. Heym F. Hofmann Ch. Hollenstein B. Joye R. Keller A. Lietti J.B. Lister F.B. Marcus J.M. Moret S. Nowak J. O'Rourke A. Pochelon W. Simm	Non-linear antenna loading measurements in TCA Proc. 4th Int. Symposium on Heating in Toroidal Plasmas, Rome, Italy, March 1984, Vol. I, p. 193 - 200
87	K. Appert A. de Chambrier G.A. Collins P.A. Duperrex A. Heym F. Hofmann Ch. Hollenstein B. Joye R. Keller A. Lietti J.B. Lister F.B. Marcus J.-M. Moret S. Nowak A. Pochelon W. Simm	Discontinuous heating behaviour observed in the TCA Tokamak and its interpretation in terms of the Alfvén wave spectrum Proc. 4th Int. Symposium on Heating in Toroidal Plasmas, Rome, Italy, March 1984, Vol. I, p. 171 - 178

99	A. de Chambrier G.A. Collins P.A. Duperrex A. Heym F. Hofmann Ch. Hollenstein B. Joye R. Keller A. Lietti J.B. Lister F.B. Marcus J.M. Moret A. Pochelon W. Simm S. Nowak J. O'Rourke	Magnetic turbulence measurements and confinement in the TCA Tokamak Proc. 1984 Int. Conference on Plasma Physics, Lausanne, Switzerland, June/July 1984, Vol. I, p. 75
101	K. Appert A. de Chambrier G.A. Collins P.A. Duperrex A. Heym F. Hofmann Ch. Hollenstein B. Joye R. Keller A. Lietti J.B. Lister F.B. Marcus J.-M. Moret S. Nowak A. Pochelon W. Simm	Effects of the Alfvén wave spectrum in heating experiments in TCA Proc. 1984 Int. Conference on Plasma Physics, Lausanne, Switzerland, June/July 1984, invited paper
105	A. de Chambrier G.A. Collins P.A. Duperrex A. Heym F. Hofmann Ch. Hollenstein B. Joye R. Keller A. Lietti J.B. Lister F.B. Marcus J.M. Moret S. Nowak A. Pochelon W. Simm	Alfvén wave heating - Advances in TCA 10th Int. Conf. on Plasma Physics and Controlled Nuclear Fusion Research, London, U.K., Sept. 1984

116	A. De Chambrier A. Heym F. Hofmann B. Joye R. Keller A. Lietti J.B. Lister A. Pochelon W. Simm	The experimental discovery of Discrete Alfvén Waves (DAW) in the TCA Tokamak Société Suisse de Physique, session d'automne, Octobre 1982
117	A. De Chambrier A. Heym F. Hofmann B. Joye R. Keller A. Lietti J.B. Lister A. Pochelon W. Simm	Mesure de température ionique par analyse de particule neutre dans TCA (Tokamak Chauffage Alfvén) Société Suisse de Physique, session d'automne, Octobre 1982
119	A. De Chambrier A. Heym F. Hofmann B. Joye R. Keller A. Lietti J.B. Lister S. Nowak A. Pochelon W. Simm	Bilan d'énergie durant le chauffage Alfvén dans le Tokamak TCA de Lausanne Société Suisse de Physique, session d'automne, Octobre 1982
137	B. Joye A. de Chambrier G.A. Collins A. Heym F. Hofmann Ch. Hollenstein R. Keller A. Lietti J.B. Lister S. Nowak J. O'Rourke N.J. Peacock A. Pochelon M.F. Stamp W. Simm	Mesures spectroscopiques du plasma du Tokamak TCA Société Suisse de Physique, Session de printemps, Mars 1983

138	S. Nowak A. de Chambrier G.A. Collins A. Heym F. Hofmann Ch. Hollenstein B. Joye R. Keller A. Lietti J.B. Lister J. O'Rourke A. Pochelon W. Simm	Verunreinigungsstrahlung des Tokamak TCA Société Suisse de Physique, Session de printemps, Mars 1983
139	A. de Chambrier G.A. Collins A. Heym F. Hofmann Ch. Hollenstein B. Joye R. Keller A. Lietti J.B. Lister S. Nowak J. O'Rourke A. Pochelon W. Simm	Mesure de flux de neutres lors de déplacement du plasma TCA Société Suisse de Physique, Session de printemps, Mars 1983
140	J.M. Moret A. de Chambrier G.A. Collins A. Heym F. Hofmann Ch. Hollenstein B. Joye R. Keller A. Lietti J.B. Lister S. Nowak J. O'Rourke A. Pochelon W. Simm	Etude paramétrique de décharges ohmiques dans le Tokamak TCA Société Suisse de Physique, Session de printemps, Mars 1983
141	P.A. Duperrex A. de Chambrier G.A. Collins A. Heym F. Hofmann Ch. Hollenstein B. Joye R. Keller A. Lietti J.B. Lister S. Nowak J. O'Rourke A. Pochelon W. Simm	Caractérisation de la turbulence magnétique sur TCA Société Suisse de Physique, Session de printemps, Mars 1983

142 R. Keller
A. de Chambrier
G.A. Collins
A. Heym
F. Hofmann
Ch. Hollenstein
B. Joye
A. Lietti
J.B. Lister
S. Nowak
J. O'Rourke
A. Pochelon
W. Simm

Identification des modes d'ondes d'Alfvén
Société Suisse de Physique, Session de Printemps, Mars 1983

143 A. Pochelon
A. de Chambrier
G.A. Collins
A. Heym
F. Hofmann
Ch. Hollenstein
B. Joye
R. Keller
A. Lietti
J.B. Lister
S. Nowak
J. O'Rourke
W. Simm

Le Tokamak TCA (CRPP-EPFL)
Société Suisse de Physique, Session de printemps, Mars 1983

148A A. de Chambrier
P.A. Duperrex
M. Grossmann
A. Heym
F. Hofmann
Ch. Hollenstein
B. Joye
R. Keller
A. Lietti
J.B. Lister
F.B. Marcus
J.M. Moret
S. Nowak
J. O'Rourke
A. Pochelon
W. Simm

Experiments with DC polarisation on the RF-antennae of the TCA tokamak
Société Suisse de Physique, Session de printemps, Mars 1984

160	LRP 212/82	A. de Chambrier P.A. Dupperex A. Heym F. Hofmann B. Joye R. Keller A. Lietti J.B. Lister A. Pochelon W. Simm	Observation of fast current fluctuations during internal disruptions in TCA, by using Alfvén wave diagnostics
164	LRP 216/82	A. de Chambrier A. Heym F. Hofmann B. Joye R. Keller A. Lietti J.B. Lister P.D. Morgan N.J. Peacock A. Pochelon M.F. Stamp	Measurements of electron and ion heating by Alfvén waves in the TCA Tokamak
167	LRP 219/83	F. Hofmann B. Joye	Plasma equilibrium in the TCA Tokamak
168	LRP 220/83	M.F. Stamp A. Pochelon N.J. Peacock J.B. Lister B. Joye H. Gordon	A specroscopic survey of the TCA Tokamak with and without low-frequency rf heating
174	LRP 226/83	J.K. Gimzewski F. Hofmann Ch. Hollenstein B. Joye A. Lietti J.B. Lister A. Pochelon S. Veprek	Scrape-off measurements during Alfvén wave heating in the TCA Tokamak

178	LRP 232/83	R. Behn A. de Chambrier G.A. Collins P.A. Duperrex A. Heym F. Hofmann Ch. Hollenstein B. Joye R. Keller A. Lietti J.B. Lister J.-M. Moret S. Nowak J. O'Rourke A. Pochelon W. Simm	Recent Alfvén wave heating results
181	LRP 236/84	F. Hofmann K. Appert L. Villard	Optimization of antennae for Alfvén wave heating in the TCA Tokamak
182	LRP 237/84	A. de Chambrier G.A. Collins P.A. Duperrex A. Heym F. Hofmann Ch. Hollenstein B. Joye R. Keller A. Lietti J.B. Lister F.B. Marcus J.-M. Moret S. Nowak A. Pochelon W. Simm S. Veprek	Effect of the heating on edge parameters in the TCA Tokamak

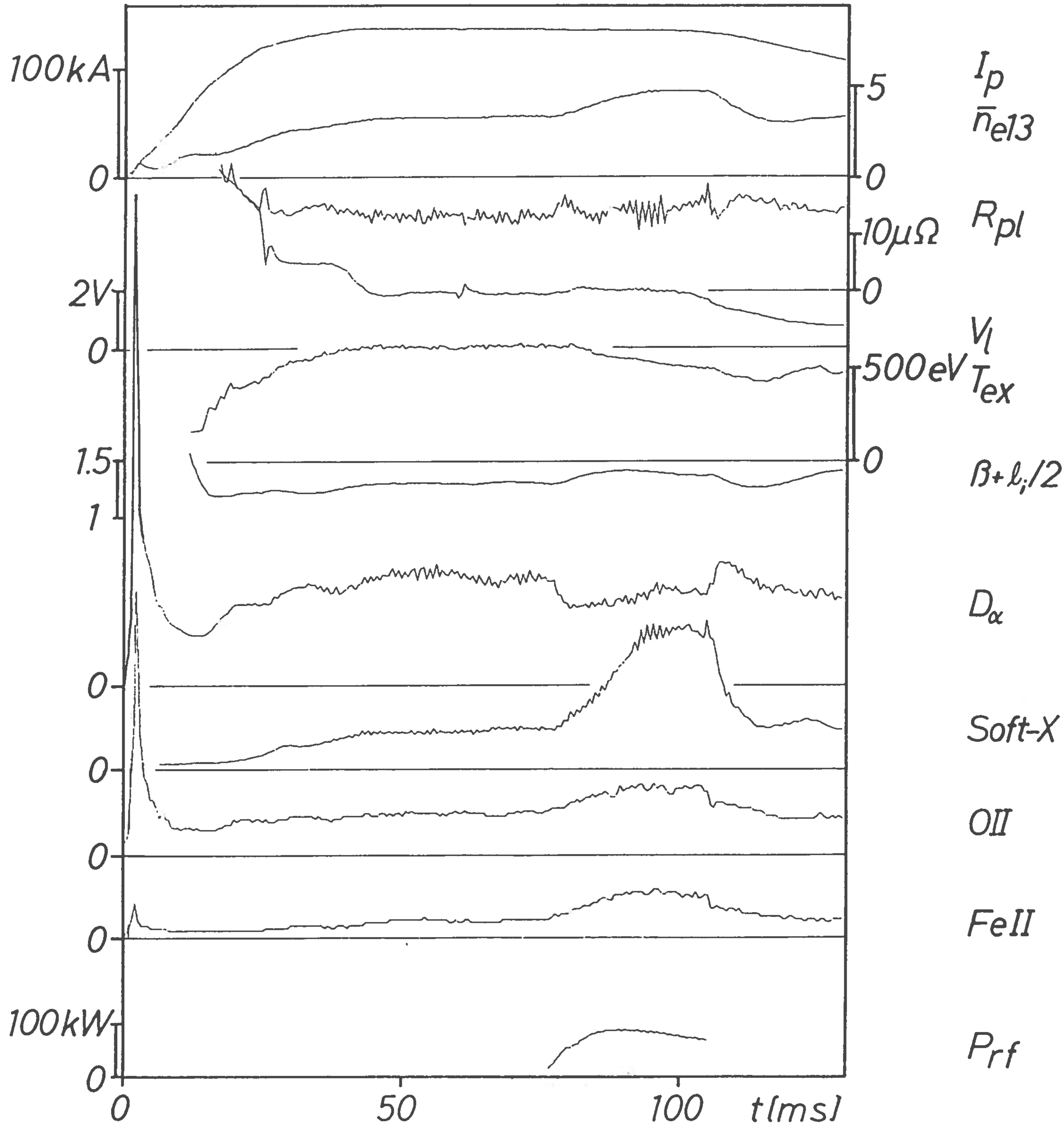
100kA
0
I_p
$\bar{n}_{e13}$
5
0
R_{pl}
10μΩ
0
2V
0
V_l
500eV
T_{ex}
0
1.5
1
β+ℓᵢ/2
D_α
0
Soft-X
0
OII
0
FeII
0
100kW
0
P_{rf}
0
50
100
t(ms)

FIGURE 1

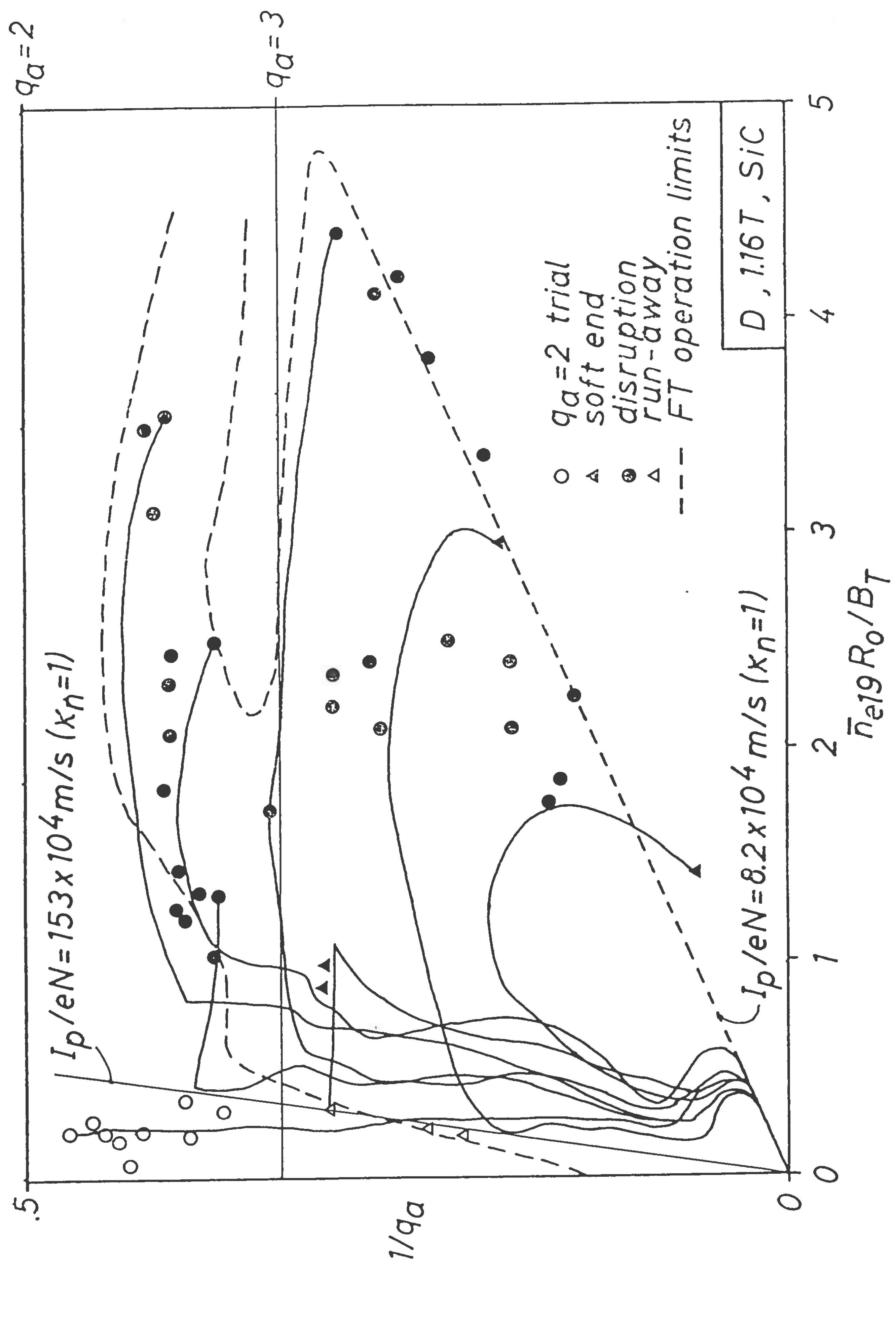

q_a = 2
q_a = 3
I_p/eN=153x10^4 m/s (κ_n=1)
I_p/eN=8.2x10^4 m/s (κ_n=1)
q_a=2 trial
soft end
disruption
run-away
FT operation limits
D , 1.16T , SiC
.5
1/q_a
0
0
1
2
3
4
5
n̄_e19 R_o/B_T

FIGURE 2

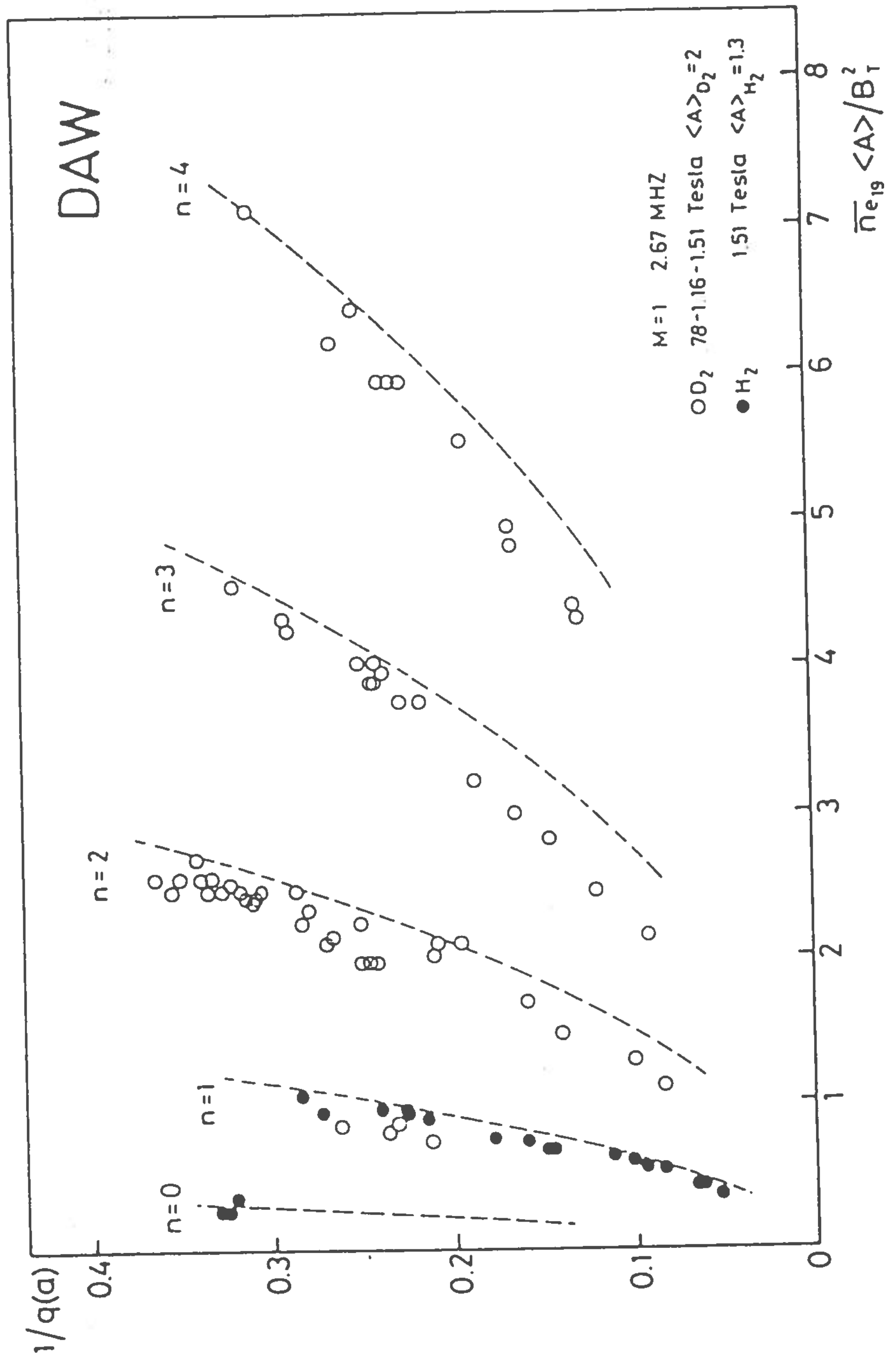
DAW
n = 0
n = 1
n = 2
n = 3
n = 4
M = 1 2.67 MHZ
○ D_2 78-1.16-1.51 Tesla $\langle A \rangle_{D_2} = 2$
● H_2 1.51 Tesla $\langle A \rangle_{H_2} = 1.3$
1/q(a)
0.4
0.3
0.2
0.1
0
1
2
3
4
5
6
7
8
$\overline{n}_{e_{19}} \langle A \rangle / B_T^2$

FIGURE 5

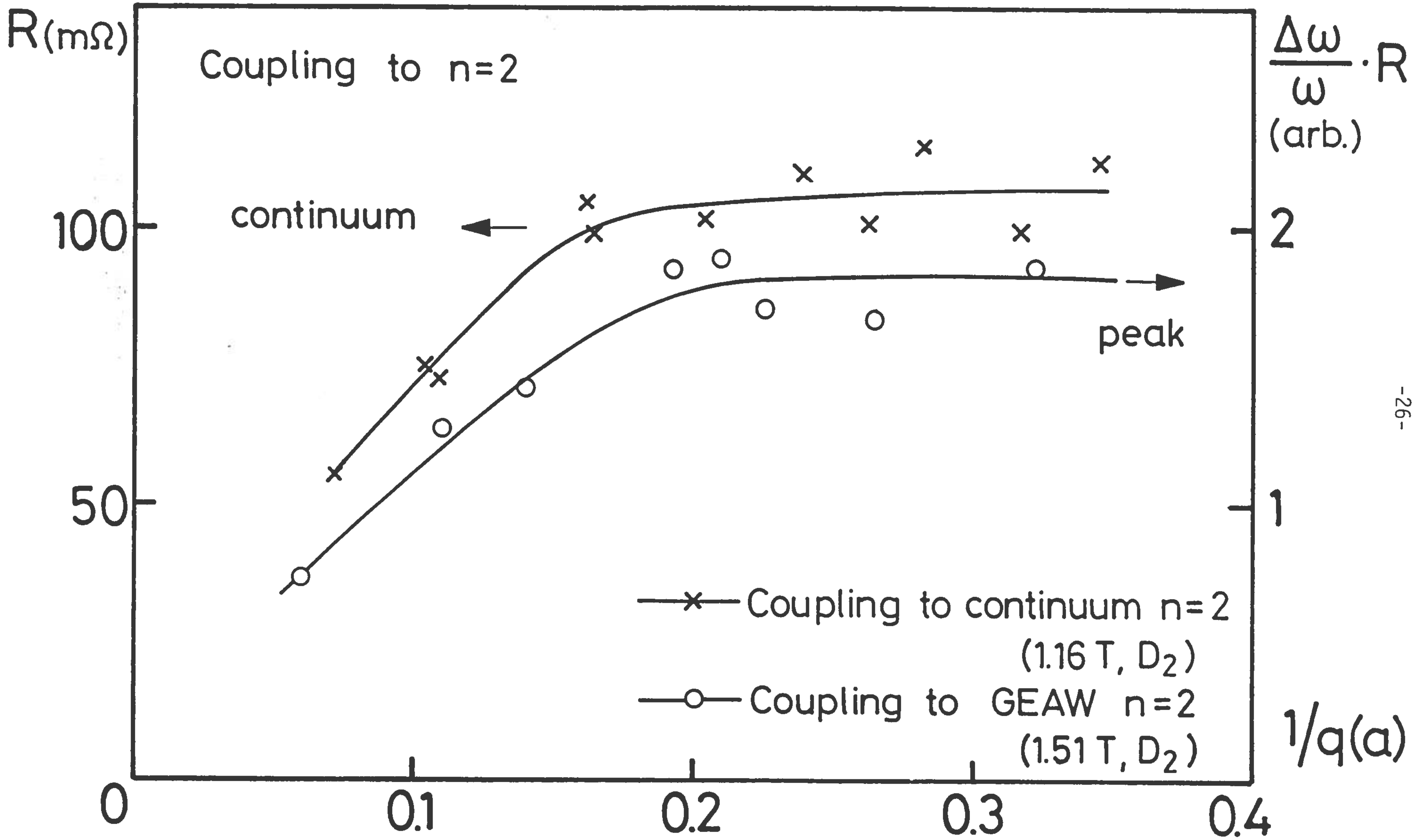

R(mΩ)
Coupling to n=2
continuum
peak
$\frac{\Delta\omega}{\omega} \cdot R$ (arb.)
100
50
0
2
1
0.1
0.2
0.3
0.4
1/q(a)
Coupling to continuum n=2 (1.16 T, D_2)
Coupling to GEAW n=2 (1.51 T, D_2)

FIGURE 6

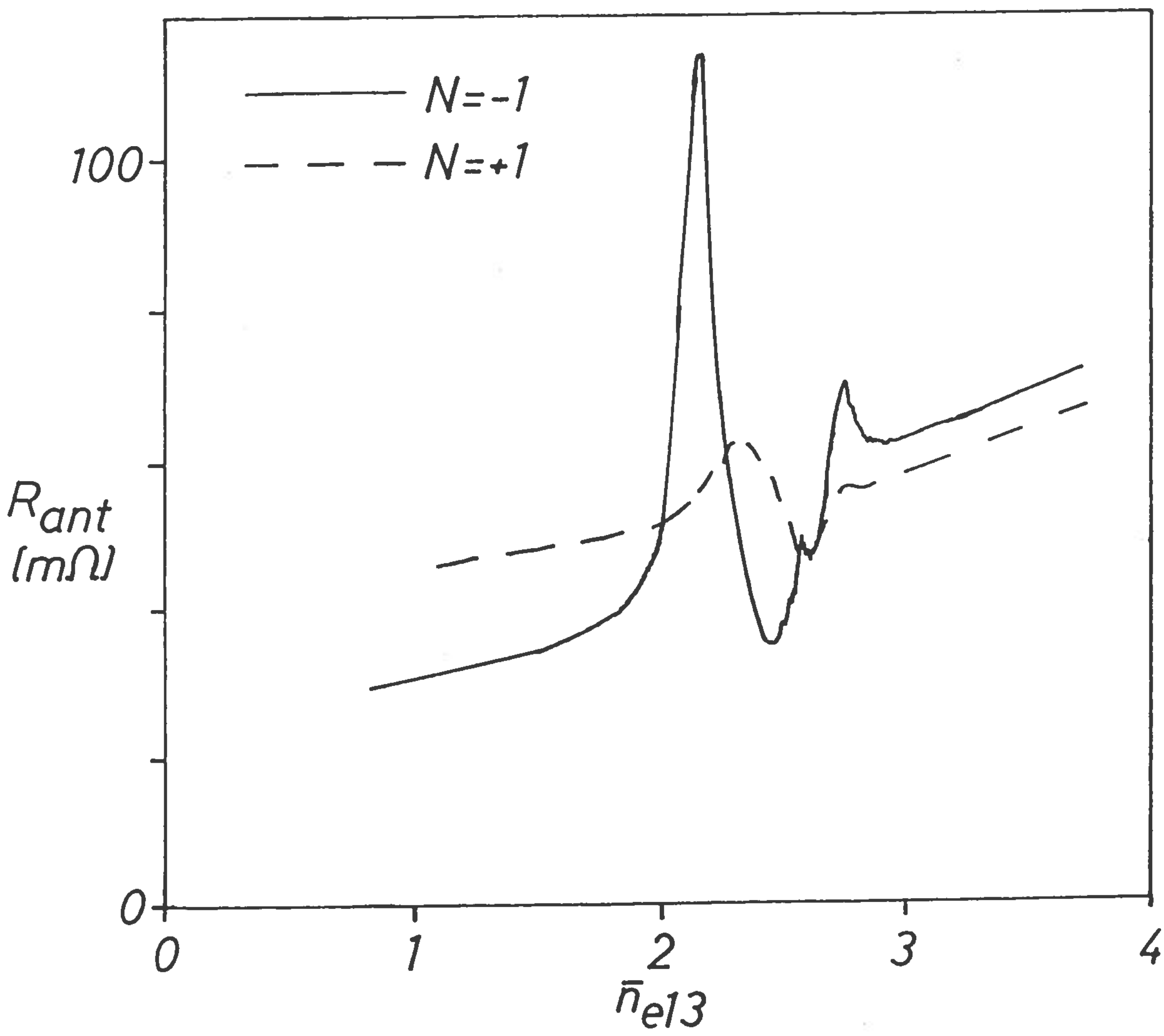

FIGURE 7

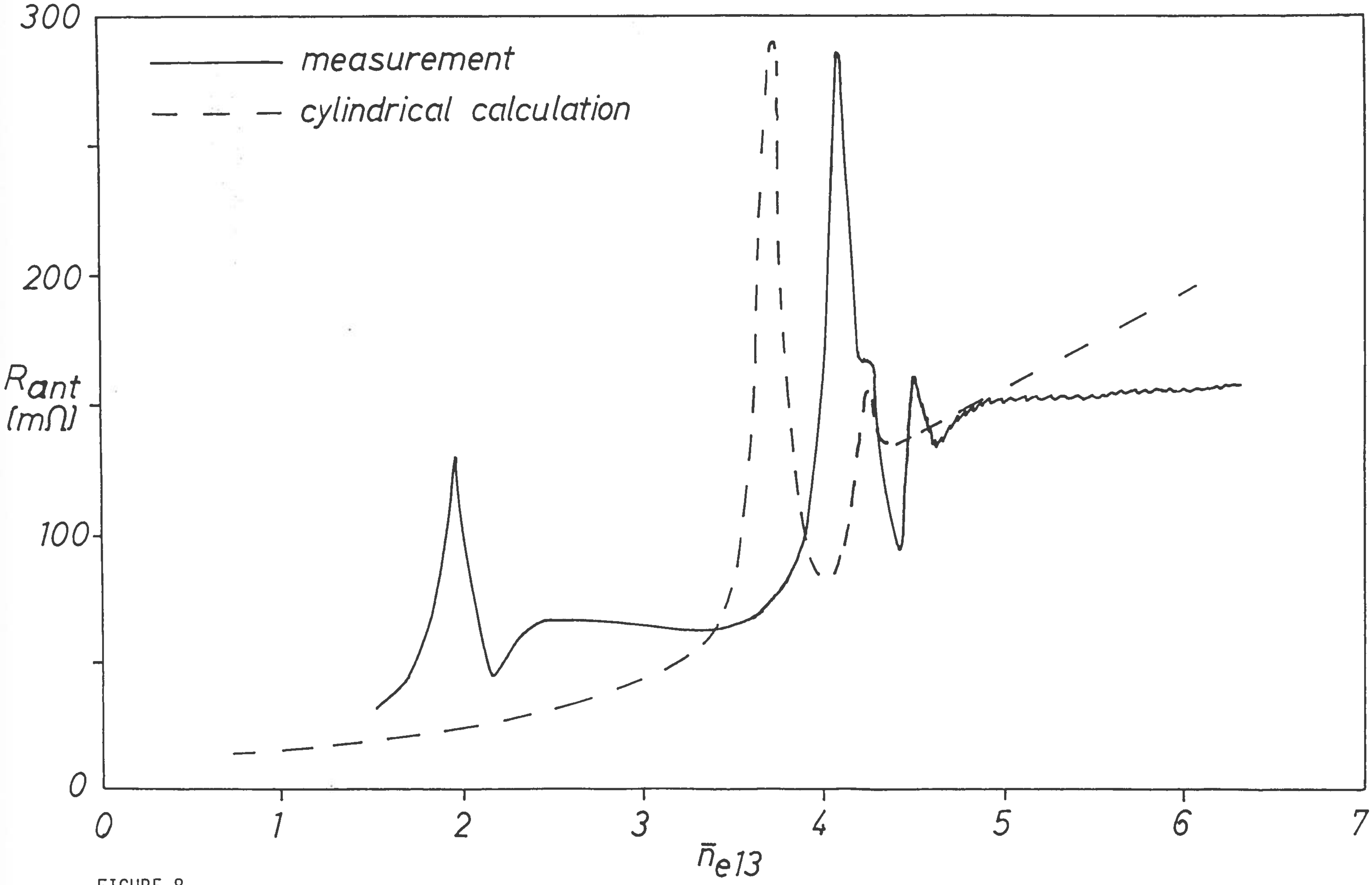
measurement
cylindrical calculation
300
200
100
0
Rant
(mΩ)
0
1
2
3
4
5
6
7
n̄e13

FIGURE 8

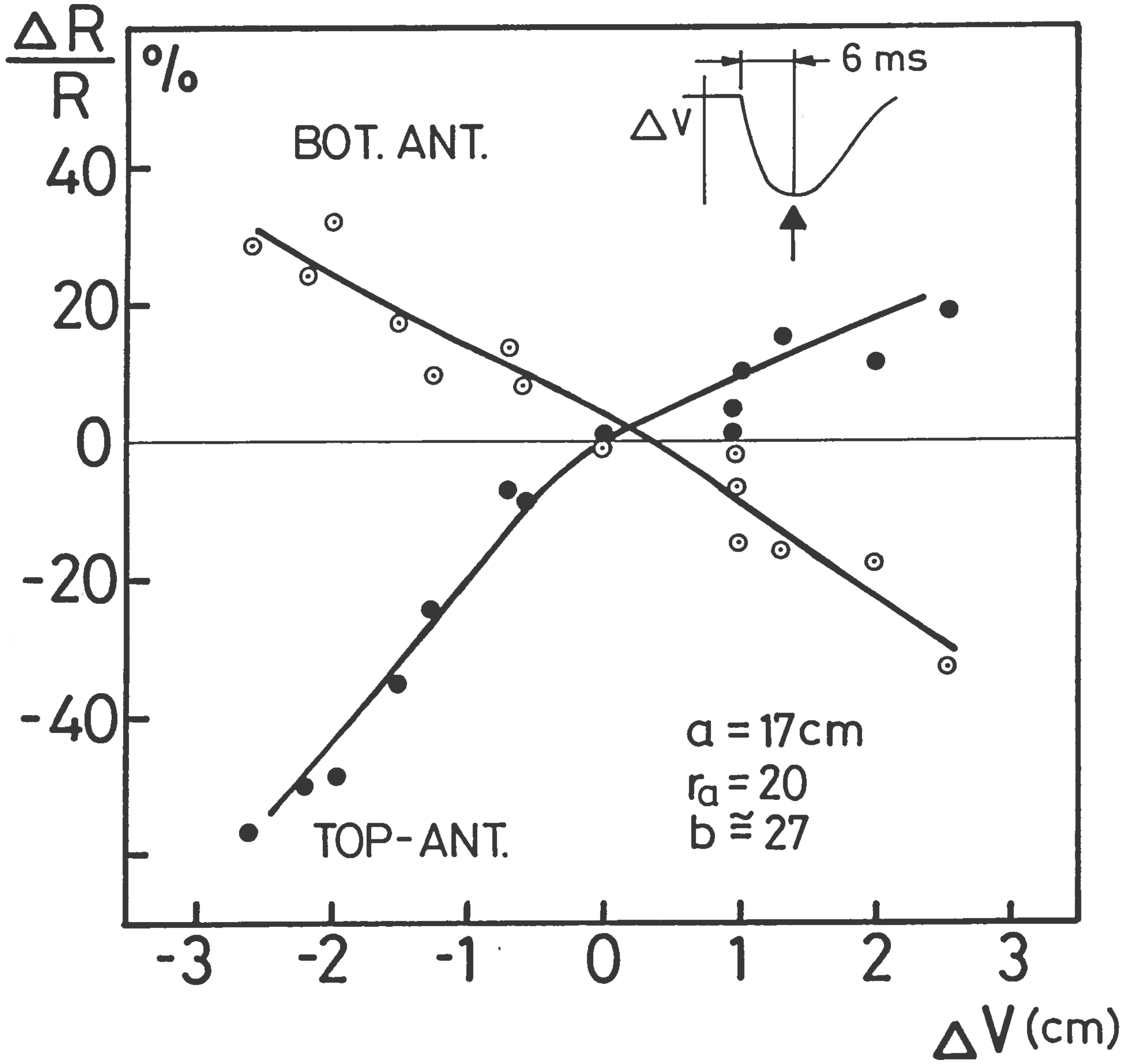
ΔR/R %
BOT. ANT.
TOP-ANT.
6 ms
ΔV
40
20
0
-20
-40
a = 17cm
ra = 20
b ≅ 27
-3
-2
-1
0
1
2
3
ΔV (cm)

FIGURE 9

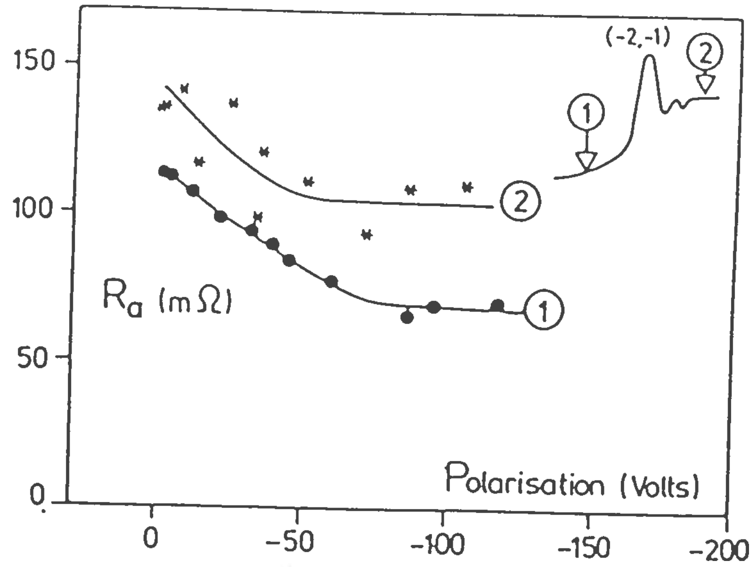
150
100
50
0
(-2,-1)
2
1
R_a (mΩ)
Polarisation (Volts)
0
-50
-100
-150
-200

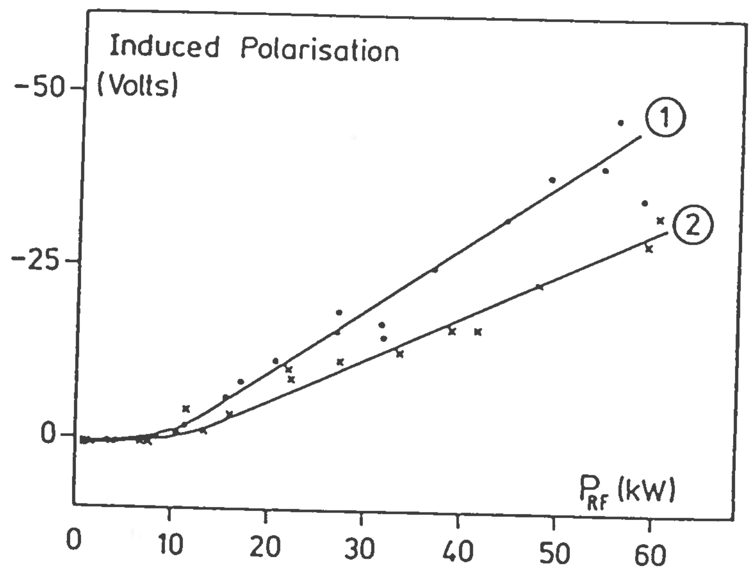
Induced Polarisation
(Volts)
-50
-25
0
1
2
P_{RF} (kW)
0
10
20
30
40
50
60

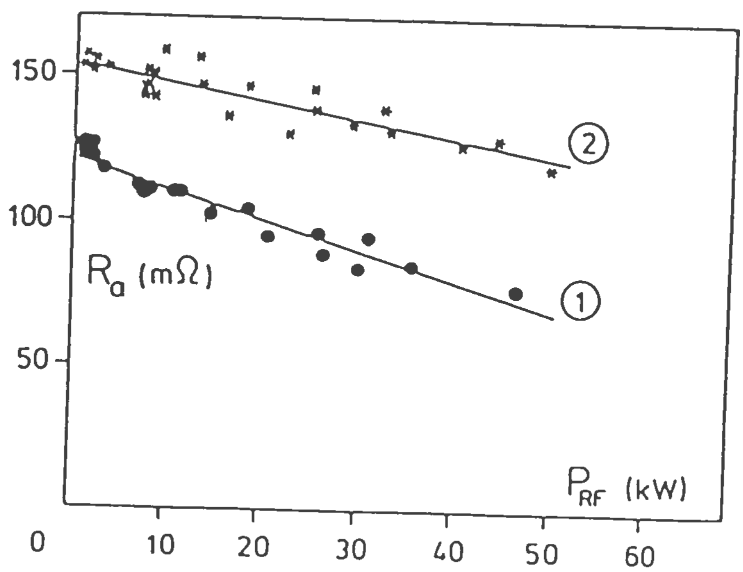
150
100
50
2
1
R_a (mΩ)
P_{RF} (kW)
0
10
20
30
40
50
60

FIGURE 10

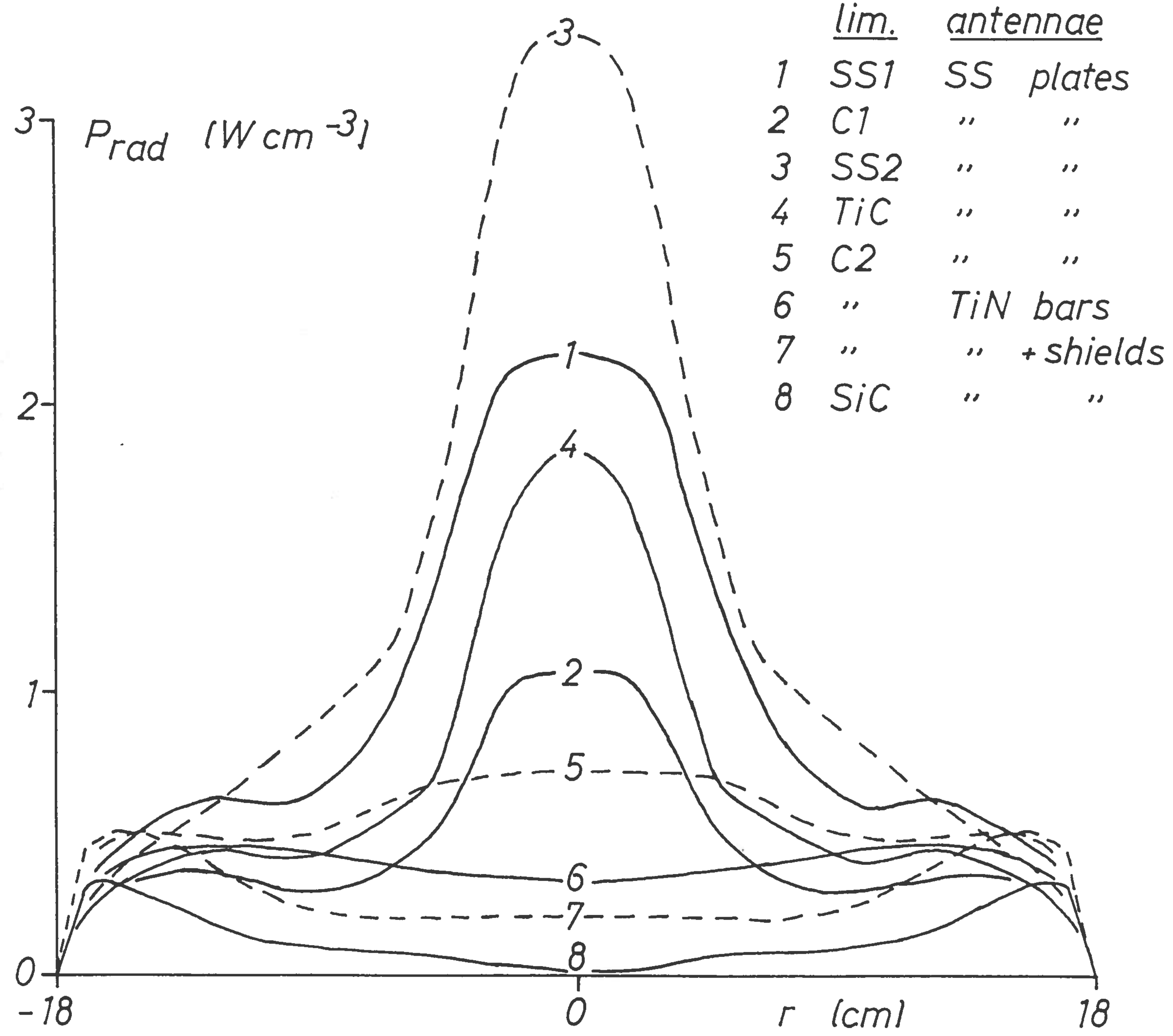
P_{rad} (W cm^{-3})
3
2
1
0
-18
0
18
r (cm)
1
4
2
5
6
7
8
3
lim. antennae
1 SS1 SS plates
2 C1 " "
3 SS2 " "
4 TiC " "
5 C2 " "
6 " TiN bars
7 " " +shields
8 SiC " "

FIGURE 11

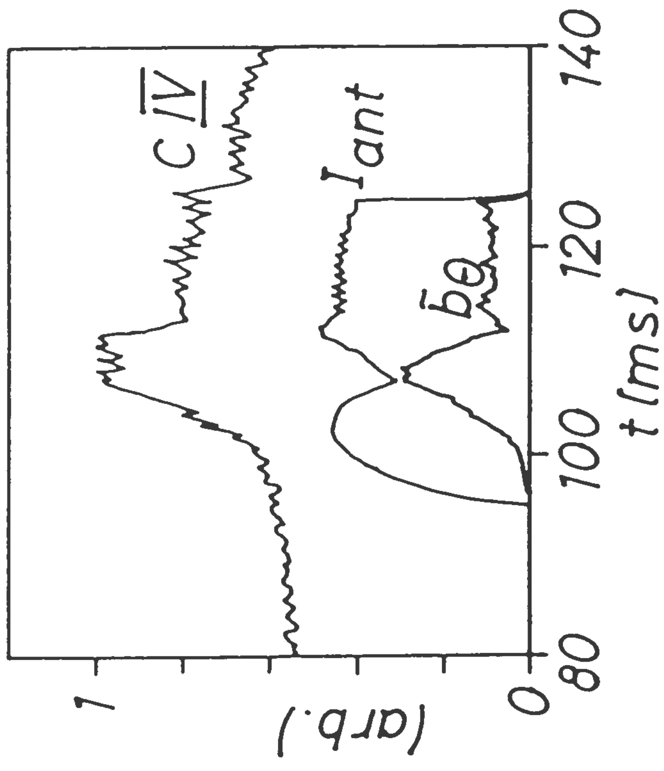

FIGURE 12

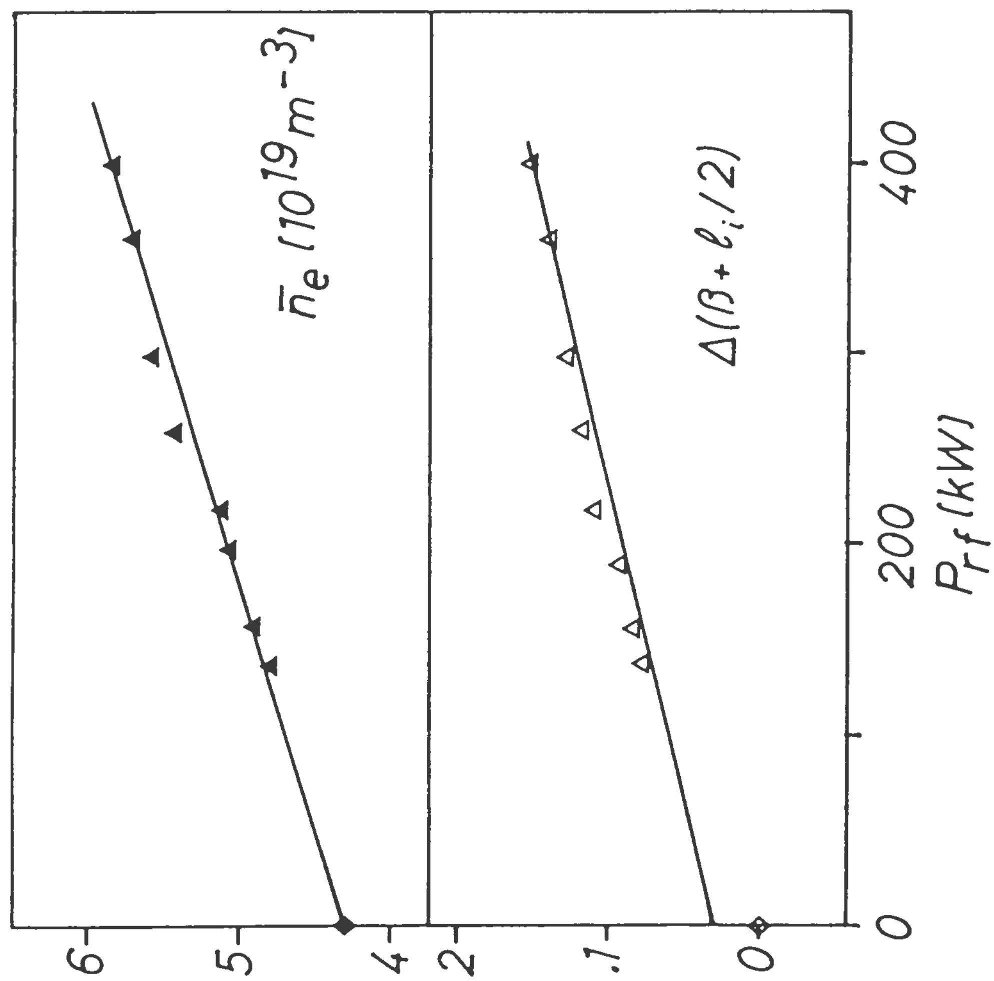

FIGURE 13

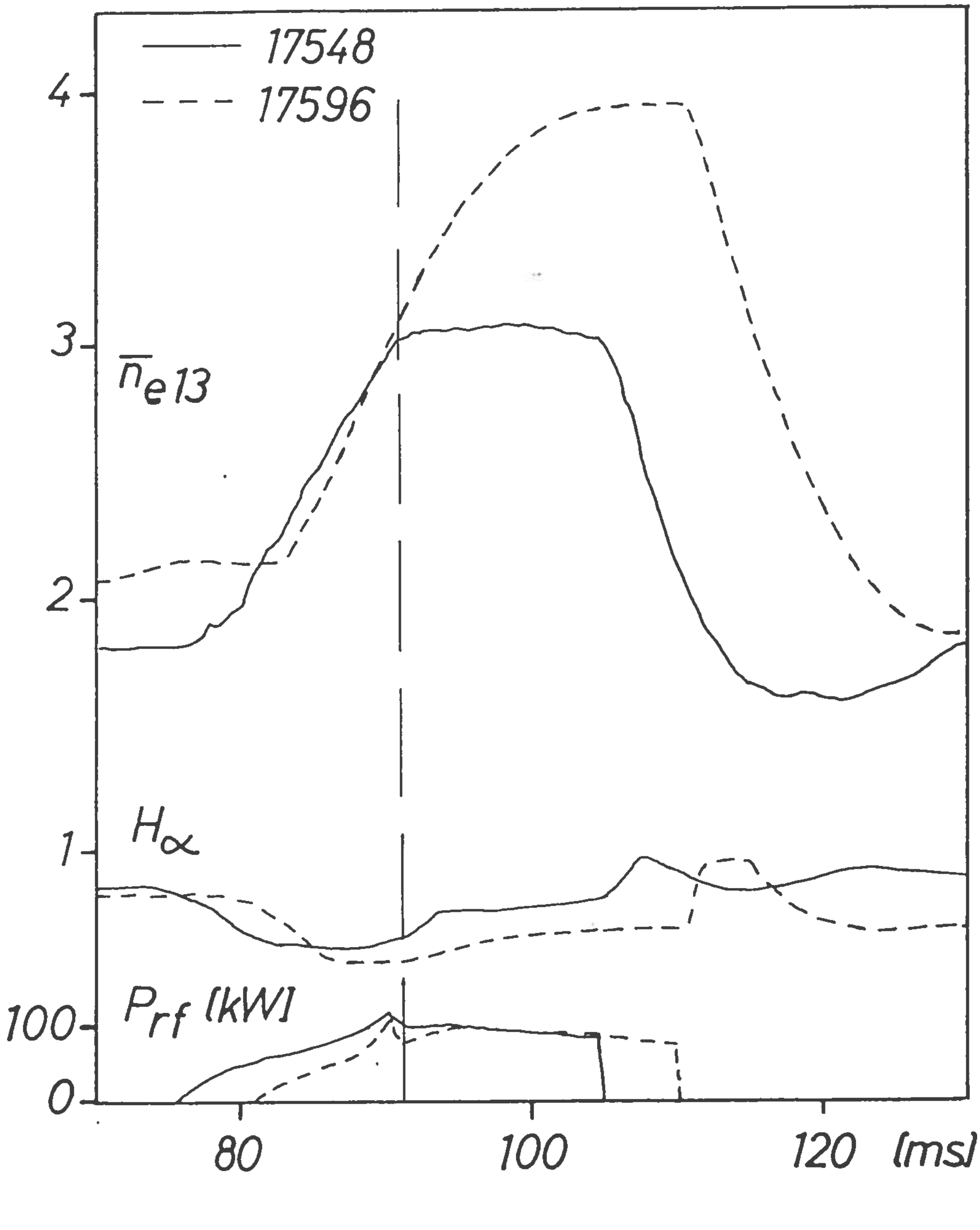

FIGURE 14

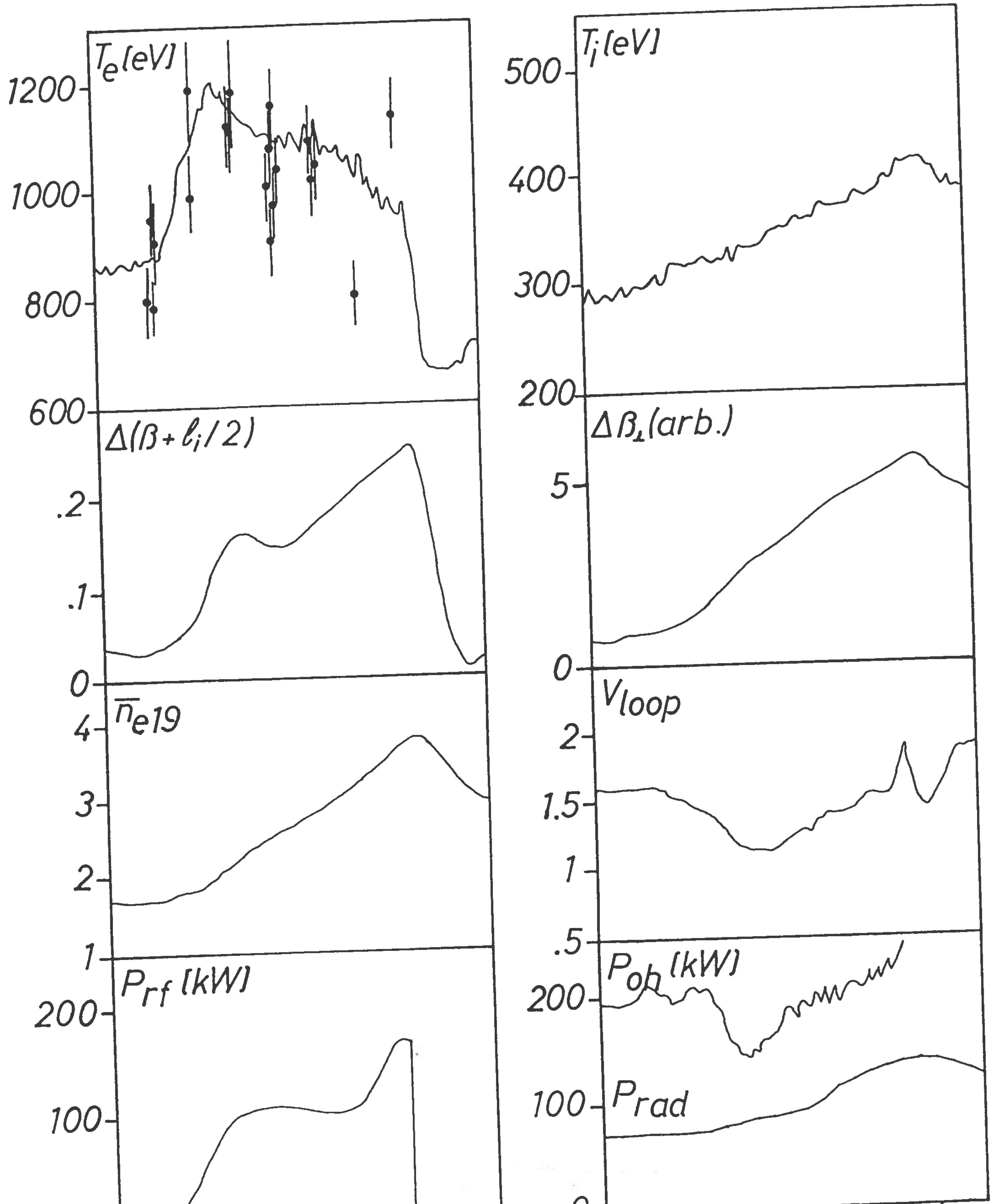

T_e [eV]
1200
1000
800
600
$\Delta(\beta+\ell_i/2)$
.2
.1
0
$\bar{n}_{e19}$
4
3
2
1
P_{rf} [kW]
200
100
0
60
80
100
t [ms]
T_i [eV]
500
400
300
200
$\Delta\beta_\perp$(arb.)
5
0
V_{loop}
2
1.5
1
.5
P_{oh} [kW]
200
100
P_{rad}
0
60
80
100
t [ms]

FIGURE 15